Penerbit Akademia Baru

CFD Letters

Journal homepage: www.akademiabaru.com/cfdl.html
ISSN: 2180-1363

Effect of Contact Angle on Meniscus Evolution and Contact Line Jump of Underfill Fluid Flow in Flip-Chip Encapsulation

Open Access

Fei Chong Ng[1], Lun Hao Tung[1], Mohd Hafiz Zawawi[2], Muhamed Abdul Fatah Muhamed Mukhtar[3], Mohamad Aizat Abas[1,*], Mohd Zulkifly Abdullah[1]

[1] School of Mechanical Engineering, Universiti Sains Malaysia, Engineering Campus, Nibong Tebal, 14300, Penang, Malaysia
[2] Department of Civil Engineering, College of Engineering, Universiti Tenaga Nasional (UNITEN), Kajang, 43000, Selangor, Malaysia
[3] Faculty of Engineering, DRB-Hicom University of Automotive Malaysia, 26607, Pekan, Pahang, Malaysia

ARTICLE INFO

Article history:
Received 19 April 2020
Received in revised form 17 June 2020
Accepted 23 June 2020
Available online 29 June 2020

ABSTRACT

Despite the contact angle of underfill fluid is largely correlated to the flowability, it was scarcely being investigated in the design optimization of flip-chip underfill encapsulation process. Furthermore, the detailed implication of the variation of contact angle on the flow mechanism was never being discussed. Thus, this paper is devoted to study the variation effect of contact angle on both spatial aspects of meniscus evolution and contact line jump of underfill flow menisci. The governing analytical equations that describe both meniscus evolution and contact line jump were well-validated with the past experimental and numerical findings. It was revealed that the bump contact angle critically determined the separation between concave and convex menisci. Generally, larger bump contact angle yields the earlier formation of convex menisci that is nearer to the bump entrant. Consequently, the occurrence of convex menisci in the bump region increased for the case of high bump contact angle. Moreover, when the contact angle increases, the equilibrium positions of entrant jump meniscus locates nearer to the bump entrant; while the equilibrium meniscus of exit jump becomes further away from the bump exit. These findings provided microscopic insights of the influence of contact angle on the characteristic and dynamic of flow menisci upon interacting with the solder bump array, which may benefit both electronic packaging and microfluidics sectors in general.

Keywords:
Contact angle; Contact line jump; Electronic Packaging; Flip chip; Meniscus; Underfill encapsulation

1. Introduction

Underfill encapsulation process is conducted in the electronic packaging and manufacturing assembly sectors to improve both the reliability and performance of flip-chip package [1-2]. During the flip-chip underfill process, a highly viscous epoxy-like mixture with fillers loaded known as the underfill fluid [3] is gradually dispended into the small gap beneath the chip and substrate, as

* *Corresponding author.*
E-mail address: aizatabas@usm.my (Mohamad Aizat Abas)

https://doi.org/10.37934/cfdl.12.6.2838

depicted in Figure 1. The solder bumps array would partially obstruct the capillary flow of underfill fluid. The chip assembly was cured thereafter in order for the underfill fluid become harden and fully encapsulated the gap beneath the chip and the substrate. Primarily, the underfill encapsulation process relieved the residual stress due to thermal mismatch while protecting the solder joints in the flip-chips [1-4].

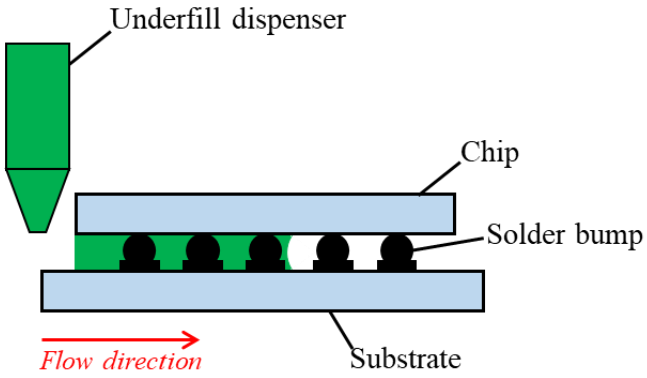

Fig. 1. Schematic of flip-chip underfill encapsulation process [3]

In the past, there are various research works conducted to optimize the underfill process through package design [5-12] as well as to resolve the reliability issues of incomplete filling [13] and void defect [14-15]. In the design optimization works, various parameters were invoked to achieve the most miniature flip-chip package together with the best underfill productivity. The latter objective is to reduce the manufacturing lead time and thus to save the operating cost. The studied parameters in the underfill system includes bump pitch [5-7], gap height [8-9], bump shape [10-11] and contact angle [12]. The bump pitch is found to be the most studied variable in optimization design whereas the contact angle only being reported in only one literature [12].

Meniscus evolution is the microscopic behavior of flow meniscus upon interacting with the cylindrical bumps array, where the meniscus tends to change its shape from concave to convex in accordance to the surface force and capillarity. Such interesting behavior of underfill flow menisci in flip-chip bump array was experimentally observed by Lee *et al*., [6] and subsequently being numerically visualized by Ng *et al*., [7]. Later, this meniscus evolution phenomenon was incorporated in the development of analytical filling time models [16-19].

Meanwhile, the contact line jump (CLJ) is an interfacial phenomenon between the interaction of underfill fluid and solder bump. The jumps were observed in both bump entrant and bump exit, in which the meniscus of underfill fluid attempts to attach on the bump surface and to detach away from the bump surface respectively. It was firstly theorized by Young [20-21], which were then being experimentally observed by Lee *et al*., [6] and lastly numerically simulated by Ng *et al*., [7]. Similarly, CLJ is deduced as a crucial aspect on the underfill flow and hence also being considered in the analytical filling time models [16-19]. This is evident by the enhancement of accuracy of analytical filling time models as reported in Yao *et al*., [16] and Ng *et al*., [17-19] through the inclusions of both spatial aspects of meniscus evolution and CLJ.

Generally, the standalone analysis on both spatial aspects of meniscus evolution and contact line jump were limited in number despite their importances in determining the flow dynamics of underfill fluid. Moreover, only one literature that studied the variation effect on contact angle on the filling progression aspects [12]. To the best knowledge of authors, the variation effect of contact angle on both crucial aspects of meniscus evolution and contact line jump as intended to be achieved in the

current paper was never being reported elsewhere. Further, apart from electronic packaging, this work able to provide insights for other microfluidic and channel flow applications [22-23].

2. Analytical Spatial Formulation

2.1 Formulation of Meniscus Evolution

By geometrical analysis on the meniscus shape of underfill fluid subtended between two adjacent solder bumps, the meniscus evolution of underfill fluid upon interacting with the cylindrical bump array was analytically formulated and depicted in Figure 2. The initially concave meniscus at bump entrance as in Figure 2(i) and Figure 2(ii) would gradually evolves into the straight meniscus shown in Figure 2(iii) and lastly convex meniscus upon leaving the array, shown in Figure 2(iv). The meniscus that subtended between two adjacent bumps can be characterized based on the three parameters of arc subtended angle, γ, arc radius, R and center-line flow displacement, S, that being mathematically defined respectively in Eqs. (1), (2) and (3) as follows:

$$\gamma = \begin{cases} \pi + 2(\phi + \theta_b), & \text{for } \phi < -\theta_b, \\ \pi - 2(\phi + \theta_b), & \text{for } \phi \geq -\theta_b, \end{cases} \tag{1}$$

$$R = \frac{W - d\cos\phi}{2\sin\left(\frac{\gamma}{2}\right)}, \tag{2}$$

$$S = \frac{d}{2}(1 + \sin\phi) - R\left[1 - \cos\left(\frac{\gamma}{2}\right)\right], \tag{3}$$

where θ_b is the contact angle at bump surface, W is the bump pitch and d is the bump diameter.

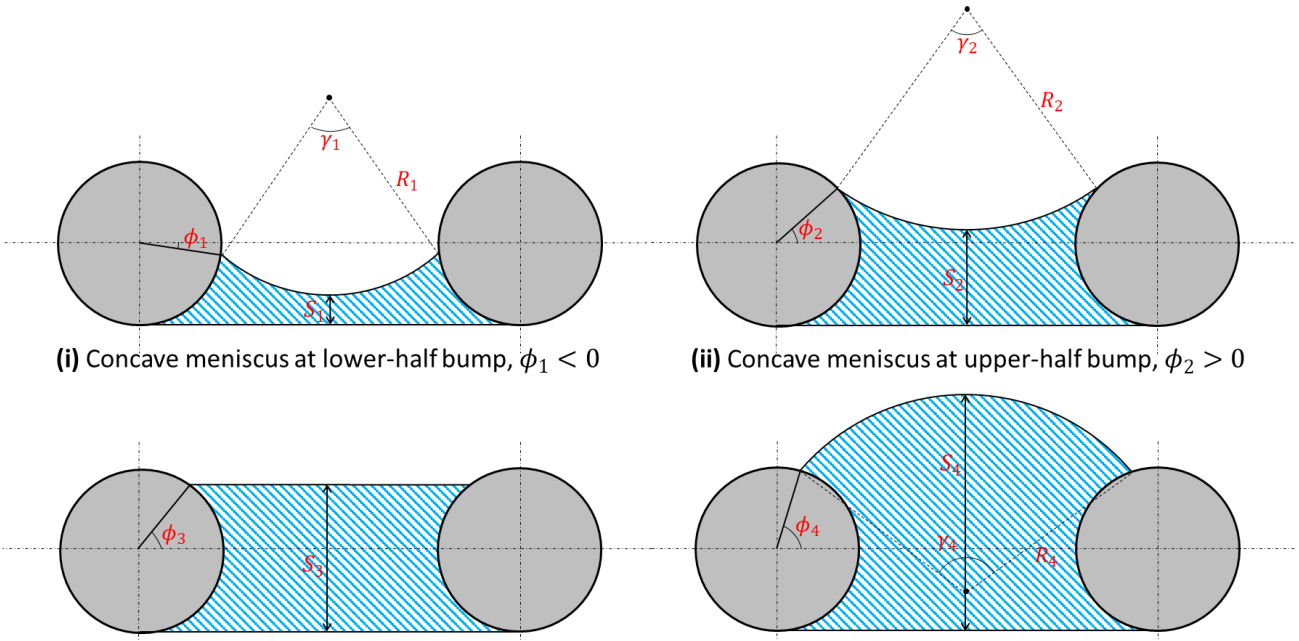

(i) Concave meniscus at lower-half bump, $\phi_1 < 0$ **(ii)** Concave meniscus at upper-half bump, $\phi_2 > 0$

(iii) Straight meniscus at upper-half bump, $\phi_3 = \frac{\pi}{2} - \theta_b$ **(iv)** Convex meniscus at upper-half bump, $\phi_4 > \frac{\pi}{2} - \theta_b$

Fig. 2. Transient evolution of flow meniscus in bump array [17-18]

2.2 Formulation of Contact Line Jump

The contact line jump (CLJ) occurred when the underfill fluid transitions to or away from, the solder bump, resulting the change in meniscus shapes at the principle plane that parallel to the flow direction. Two new CLJ criterions for the equilibrium meniscus after the jumps respectively for the flow entrance and flow exit were proposed, as illustrated in Figure 3. The angular position of equilibrium meniscus after attach jump, ϕ_j satisfies the Eq. (4):

$$\left(1+\sin\phi_j\right)=\frac{W^*-\cos\phi_j}{\cos\left(\phi_j+\theta_b\right)}\left[1+\sin\left(\phi_j+\theta_b\right)\right]. \tag{4}$$

Meanwhile, the dimensionless center-line flow displacement of the equilibrium meniscus formed after the exit CLJ is given by the Eq. (5):

$$S_j^*=1+\frac{W^*(1-\cos\theta_b)}{2\sin\theta_b}, \tag{5}$$

where the dimensionless bump pitch, $W^*=W/d$.

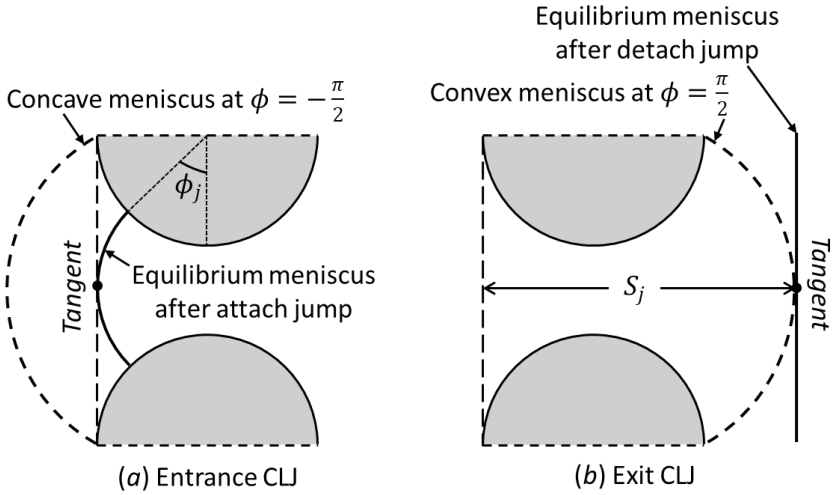

Fig. 3. Equilibrium menisci of entrance and exit contact line jumps

3. Results and Discussion

3.1 Validation

A validation study was conducted to access the veracity of proposed analytical model on meniscus evolution of underfill fluid flow in bump array, by comparing it to the experimental meniscus evolution obtained in Lee *et al.,* [6]. Figure 4 compares between the current analytical meniscus evolution with the experimental meniscus evolution [6] at the different filling instances. It was found that both the experimental and analytical menisci are comparable at four filling stages from entrance to the detach jump. Initially, the concave meniscus was formed at the entrance of bump array and it jumps instantaneously to the bump. As it approaches the bump exit, the meniscus shape changed to convex shape and gradually detached away from the bump to form a straight meniscus in the bumpless region. This had affirmed the veracity of the current analytical model as given in the Eqs. (1) to (5) on the meniscus evolution and contact line jump.

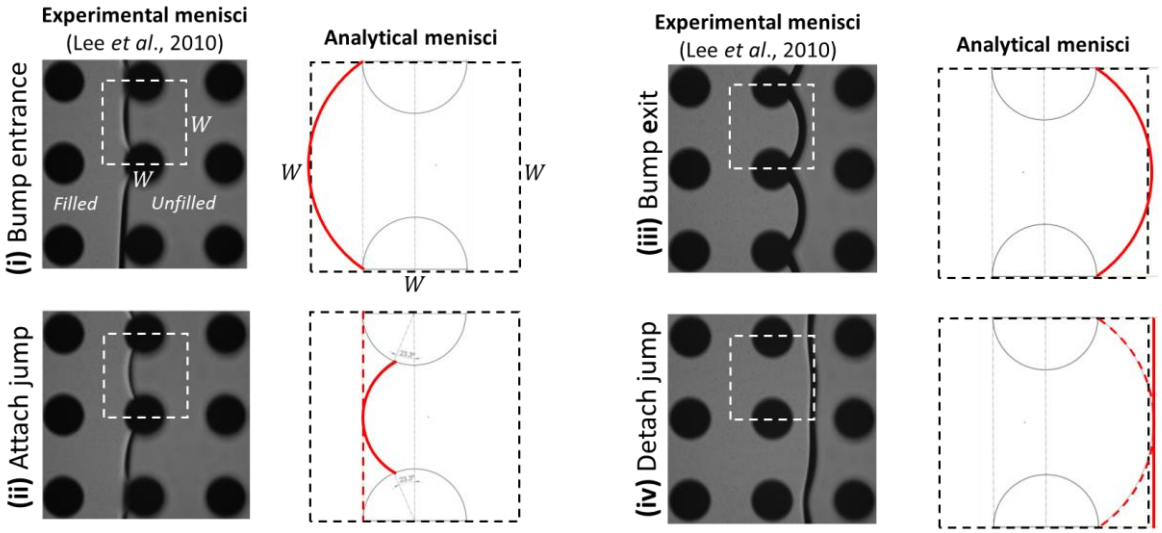

Fig. 4. Comparison of experimental [6] and analytical meniscus evolution of underfill flow

3.2 Effect of Bump Contact Angle on Meniscus Evolution

The plots in Figure 5 present the variations of meniscus spatial parameters of γ, R and S as given in Eqs. (1) to (3) with the bump contact angle, θ_b. It is revealed that the θ_b substantially affects the trends of all three spatial parameters, hence the impact of θ_b cannot be overlooked and played crucial role in the optimization works.

When increasing the value of θ_b, it is observed that the plot of γ against ϕ shifted to the left, such that both the turning point and ϕ_c decreases. Also, the asymptote of graph of R against ϕ also shifts to the left when θ_b increases. The overall effect of increasing the θ_b is the lengthening of bump region for the occurrence of convex meniscus; equivalently magnifying the bump resisting region. For $\theta_b = 75°$, the straight meniscus formed at $\phi_c = 15°$ in which the convex meniscus is observed in the thereafter bump region of angular displacement of $75°$. Comparing to perfect wetting with $\theta_b = 0°$, there is no convex meniscus is observed through the meniscus evolution in the bump region since $\phi_c = 90°$. With the occurrence of convex meniscus becoming more frequent, it is inferred that the bump resisting effect becomes more significant. This also had justified that the segmentation between bump assisting and bump resisting zones can be solely determined with the value of θ_b. On other hand, the variation of S spans in the larger range for the case of higher θ_b. This is due to the concave meniscus at bump entrance and the larger convex meniscus with higher magnitude of γ, for the case of increasing θ_b. As a result, a large θ_b causes the filling length of expansion flow for exit CLJ to be longer.

Figure 6 provides the summarized view on how the meniscus subtended between two adjacent bumps as it evolves when the θ_b is manipulated. It appears that the net effect of increasing bump contact angle is such that the size (i.e. curvature radius) of both concave and convex menisci at respective bump entrant and bump exit become bigger.

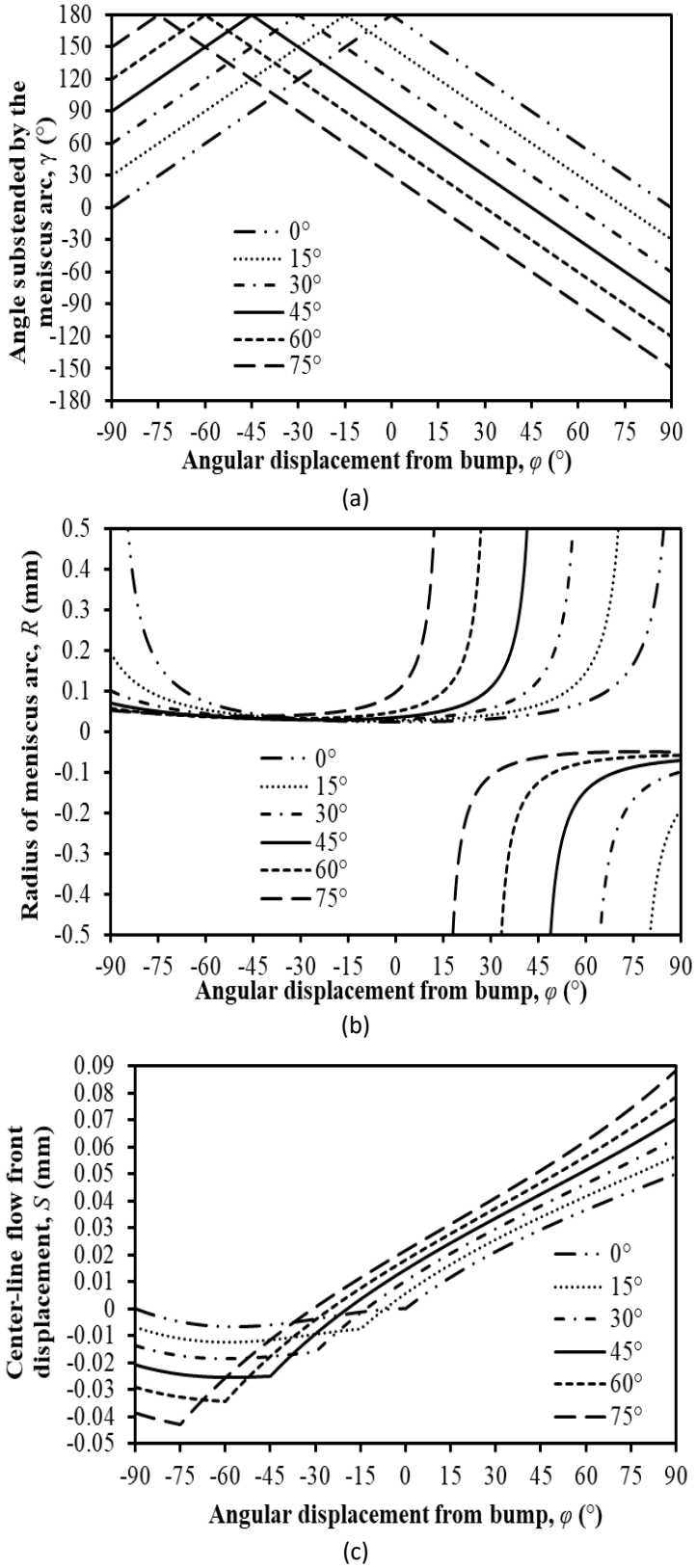

Fig. 5. Variation plots of meniscus shape parameters, (*a*) γ, (*b*) R and (*c*) S against ϕ for various bump contact angles with W = 0.10 mm and d = 0.05 mm

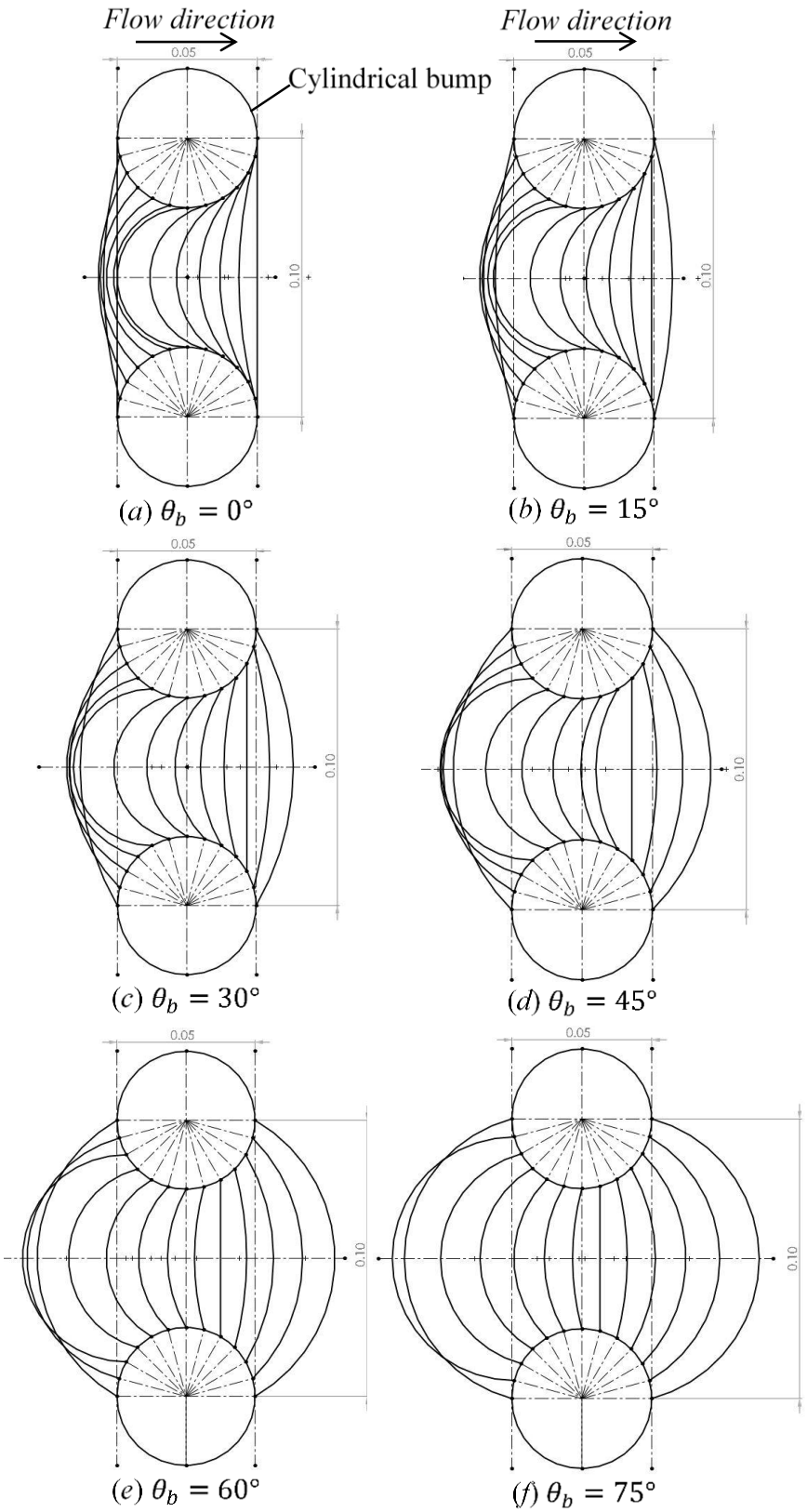

Fig. 6. Evolution of flow meniscus subtended by two adjacent cylindrical bumps with $d = 0.05$ mm and $W = 0.10$ mm but various contact angles relative to bump surface, θ_b, from the bump's angular displacement of $-90°$ to $90°$, as seen from the principal plane. The separation between each consecutive isolines is 15°

3.3 Effect of Bump Contact Angle on Contact Line Jump

Figure 7 gives the plot of angular position of equilibrium meniscus after the attach jump at various bump pitches and bump contact angles. Similarly, Figure 8 presents the variation of S_j^* together with the geometrical limitation on pitch threshold.

The common trend for both ϕ_j and S_j^* is such that they are increasing with the bump pitch. For the case of ϕ_j, longer pitch yields larger curvature radius of concave meniscus and negative center-line displacement of larger magnitude. Thus, a larger value of ϕ_j is required to attain $S = 0$. Similar reasoning is applied on the convex meniscus to explain the increasing S_j^* with W^*, which exhibits a linear relationship as shown in Eq. (5). Interestingly, the effect of bump pitch on CLJ is an opposing one at respective bump entrance and exit, which can be explained based on the flow dynamic. In the entrance where the bump is regarded as flow assisting, a larger pitch weakens the instantaneous jump. This is evident by further distance of the establishment of equilibrium meniscus and the smaller magnitude of bump capillary pressure. On the contrary, the exit CLJ is favored at larger pitch as the expansion flow to attain equilibrium meniscus is faster with lower resisting capillary.

The bump contact angle, θ_b affects the CLJ at entrance and exit in a distinct manner, where the increase in θ_b gives smaller ϕ_j but larger S_j^* for a particular pitch. Underfill fluid prefers hydrophilic bump surface and as it became more wettable (i.e. lower θ_b). The attach jump will tend to occur more instantaneously by covering larger bump region and thus giving larger ϕ_j. Furthermore, the occurrence of exit CLJ is much favorable at smaller θ_b, since the convex meniscus possess larger curvature which in turn appears like a straight meniscus. From the plot's gradients in Figure 8, it is revealed that the variation of S_j^* by W^* that is relied on θ_b. When the surface is of perfect wettability ($\theta_b = 0°$), S_j^* is independent of W^*, such that the convex meniscus does not formed as in Figure 6(*a*). Hence, the meniscus detached almost immediately away from the bump upon reaching the bump apex of $\phi = \pi/2$ and the expansion flow does not occur.

To conclude, the entrance attach jump can be enhanced by decreasing the bump pitch and bump contact angle. Meanwhile, the exit detach jump is promoted by increasing the bump pitch but decreasing the bump contact angle. Upon straightforwardly shown that the fluid with low contact angle yields quick attach jump and fast expansion flow, however the bump pitch needs to be optimized to achieve an acceptable pace of both detach and attach jumps.

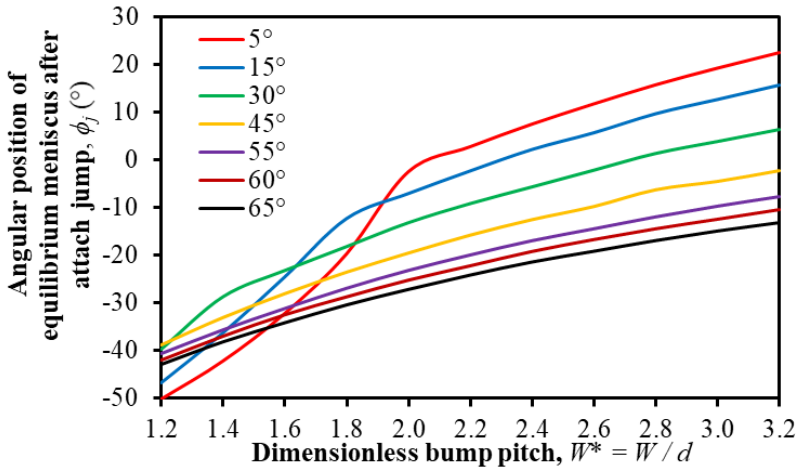

Fig. 7. Plot of the angular position of equilibrium meniscus after the attach jump (entrance CLJ) for various pitches and bump contact angles

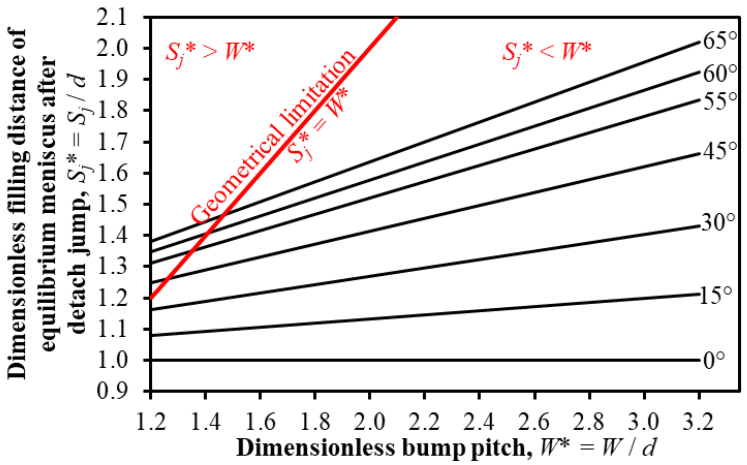

Fig. 8. Plot of the dimensionless filling distance of the equilibrium meniscus after the detach jump (exit CLJ) for various pitches and bump contact angles, together with the segmentations due to geometrical limitation

4. Conclusions

This paper provided microscopic insights on the variation effect of bump contact angle on the flow meniscus of underfill fluid during the flip-chip encapsulation process. Particularly, the impacts on both the meniscus evolution and contact line jump of underfill fluid flow were securitized based on the well-established analytical spatial flow menisci models. The bump contact angle is found to be the sole parameter that determine the separation boundary between the formations of concave and convex menisci, equivalently the bump assisting region and the bump resisting region. Initially, at the bump entrance, the flow exhibits concave meniscus before gradually straighten at the critical displacement of $\pi/2 - \theta_b$; which forms convex meniscus thereafter as it approaches to the bump exit. It can be seen that as the bump contact angle increases, the convex meniscus which associated to resisting capillary pressure tends to form nearer to the bump entrant, thus covered more portion of bump portion. The impact on dynamics of underfill fluid flow is straightforward as convex meniscus on the bump array hindered the flow advancement, it is inferred the underfill fluid of high contact angle gives slower capillary flow and equivalently longer filling time. Additionally, the bump contact angle was found to affect both the entrant and exit contact line jumps. As the contact angle increases, the equilibrium meniscus of entrant jump occurred nearer to the bump entrant; while the equilibrium meniscus of exit jump occurred further away from the bump exit. The findings attained from these works not only useful for the package design and optimization works in the electronic packaging, but as well in the microfluidic sector which involving the Stokes flow in micro-array.

Acknowledgement
This research work was partly funded by the Research University (RU) grant (Grant No.: 8014071). The authors also like to acknowledge the USM Fellowship Award, provided by Institute of Postgraduate Studies (IPS), University Sains Malaysia (USM).

References

[1] Zhang, Zhuqing, and C. P. Wong. "Recent advances in flip-chip underfill: materials, process, and reliability." *IEEE transactions on advanced packaging* 27, no. 3 (2004): 515-524. https://doi.org/10.1109/TADVP.2004.831870

[2] Ardebili, H., and M. G. Pecht. "Chapter 3-Encapsulation process technology." *Encapsulation Technologies for Electronic Applications. Elsevier* (2009): 129-79. https://doi.org/10.1016/j.ijfoodmicro.2006.07.008

[3] Ng, Fei Chong, Aizat Abas, Z. L. Gan, Mohd Zulkifly Abdullah, F. Che Ani, and M. Yusuf Tura Ali. "Discrete phase method study of ball grid array underfill process using nano-silica filler-reinforced composite-encapsulant with varying filler loadings." *Microelectronics Reliability* 72 (2017): 45-64. https://doi.org/10.1016/j.microrel.2017.03.034

[4] Ng, Fei Chong, Aizat Abas, Ismail Abustan, Z. Mohd Remy Rozainy, M. Z. Abdullah, and Sharon Melissa Kon. "Visualization of Underfill Flow in Ball Grid Array (BGA) using Particle Image Velocimetry (PIV)." In *IOP Conference Series: Materials Science and Engineering*, vol. 370, no. 1, p. 012064. IOP Publishing, 2018. https://doi.org/10.1088/1757-899X/370/1/012064

[5] Young, Wen-Bin, and Wen-Lin Yang. "The effect of solder bump pitch on the underfill flow." *IEEE Transactions on Advanced Packaging* 25, no. 4 (2002): 537-542. https://doi.org/10.1109/TADVP.2002.807564

[6] Lee, Seok Hwan, Jaeyong Sung, and Sarah Eunkyung Kim. "Dynamic flow measurements of capillary underfill through a bump array in flip chip package." *Microelectronics Reliability* 50, no. 12 (2010): 2078-2083. https://doi.org/10.1016/j.microrel.2010.07.001

[7] Ng, F. C., A. Abas, and M. Z. Abdullah. "Finite volume method study on contact line jump phenomena and dynamic contact angle of underfill flow in flip-chip of various bump pitches." In *IOP Conference Series: Materials Science and Engineering*, vol. 530, no. 1, p. 012012. IOP Publishing, 2019. https://doi.org/10.1088/1757-899X/530/1/012012

[8] Ng, Fei Chong, Mohamad Aizat Abas, M. Z. Abdullah, M. H. H. Ishak, and Gean Yuen Chong. "CUF scaling effect on contact angle and threshold pressure." *Soldering & Surface Mount Technology* 29, no. 4 (2017): 173-190. https://doi.org/10.1088/1757-899X/203/1/012013

[9] Khor, C. Y., M. Z. Abdullah, and F. Che Ani. "Underfill process for two parallel plates and flip chip packaging." *International communications in heat and mass transfer* 39, no. 8 (2012): 1205-1212. https://doi.org/10.1016/j.icheatmasstransfer.2012.07.006

[10] Ng, Fei Chong, Aizat Abas, and Mohd Zulkifly Abdullah. "Effect of solder bump shapes on underfill flow in flip-chip encapsulation using analytical, numerical and PIV experimental approaches." *Microelectronics Reliability* 81 (2018): 41-63. https://doi.org/10.1016/j.microrel.2017.12.025

[11] Khor, Chu Yee, Mohd Zulkifly Abdullah, and Wei Chiat Leong. "Fluid/structure interaction analysis of the effects of solder bump shapes and input/output counts on moulded packaging." *IEEE Transactions on Components, Packaging and Manufacturing Technology* 2, no. 4 (2011): 604-616. https://doi.org/10.1109/TCPMT.2011.2174237

[12] Young, W-B., Yang, W-L. "Underfill on Flip-Chip: The Effect of Contact Angle and Solder Bump Arrangement." *IEEE Transactions on Advanced Packaging* 29, no. 3 (2006): 647-653. https://doi.org/10.1109/TADVP.2006.879495

[13] Ng, Fei Chong, Aizat Abas, Muhammad Hafifi Hafiz Ishak, Mohd Zulkifly Abdullah, and Abdul Aziz. "Effect of thermocapillary action in the underfill encapsulation of multi-stack ball grid array." *Microelectronics Reliability* 66 (2016): 143-160. https://doi.org/10.1016/j.microrel.2016.10.001

[14] Abas, Aizat, Fei Chong Ng, Z. L. Gan, M. H. H. Ishak, M. Z. Abdullah, and Gean Yuen Chong. "Effect of scale size, orientation type and dispensing method on void formation in the CUF encapsulation of BGA." *Sādhanā* 43, no. 4 (2018): 59. https://doi.org/10.1007/s12046-018-0849-3

[15] Wang, Jinlin. "The effects of rheological and wetting properties on underfill filler settling and flow voids in flip chip packages." *Microelectronics Reliability* 47, no. 12 (2007): 1958-1966. https://doi.org/10.1016/j.microrel.2007.04.016

[16] Yao, Xing Jun, Zheng Dong Wang, and Wen Jun Zhang. "A new analysis of the capillary driving pressure for underfill flow in flip-chip packaging." *IEEE Transactions on Components, Packaging and Manufacturing Technology* 4, no. 9 (2014): 1534-1544.

https://doi.org/10.1109/TCPMT.2014.2339493

[17] Ng, Fei Chong, Aizat Abas, and M. Z. Abdullah. "Regional Segregation With Spatial Considerations-Based Analytical Filling Time Modelfor Non-Newtonian Power-Law Underfill Fluid in Flip-Chip Encapsulation." *Journal of Electronic Packaging* 141, no. 4 (2019). 041009.
https://doi.org/10.1115/1.4044817

[18] Ng, Fei Chong, Mohamad Aizat Abas, and Mohd Zulkifly Abdullah. "Filling efficiency of flip-chip underfill encapsulation process." *Soldering & Surface Mount Technology* 32, no. 1(2019).
https://doi.org/10.1108/SSMT-07-2019-0026

[19] Ng, Fei Chong, M. Yusuf Tura Ali, Aizat Abas, C. Y. Khor, Z. Samsudin, and M. Z. Abdullah. "A novel analytical filling time chart for design optimization of flip-chip underfill encapsulation process." *The International Journal of Advanced Manufacturing Technology* 105, no. 7-8 (2019): 3521-3530.
https://doi.org/10.1007/s00170-019-04573-6

[20] Young, Wen-Bin. "Capillary impregnation into cylinder banks." *Journal of colloid and interface science* 273, no. 2 (2004): 576-580.
https://doi.org/10.1016/j.jcis.2003.11.056

[21] Young, Wen-Bin. "Anisotropic behavior of the capillary action in flip chip underfill." *Microelectronics journal* 34, no. 11 (2003): 1031-1036.
https://doi.org/10.1016/j.mejo.2003.09.001

[22] Yu, Kok Hwa, Yan Xu Tan, Mohd Sharizal Abdul Aziz, Yew Heng Teoh, and Mohd Zulkifly Abdullah. "The Developing Plane Channel Flow over Water-Repellent Surface Containing Transverse Grooves and Ribs." *Journal of Advanced Research in Fluid Mechanics and Thermal Sciences* 45, no. 1 (2018): 141-148.

[23] Yu, Kok Hwa, Yew Heng Teoh, Mohd Azmi Ismail, Chih Fang Lee, and Farzad Ismail. "Numerical Investigation on the Influence of Gas Area Fraction on Developing Flow in a Pipe Containing Superhydrophobic Transverse Grooves." *Journal of Advanced Research in Fluid Mechanics and Thermal Sciences* 45, no. 1 (2018): 109-115.